dissipation provides the heating source, the temperatures in these models are derived from a balance between radiative losses and compressional heating caused by gas infalling onto the disk and moving inward toward the protostar. The disks have a surface density profile $\sigma \propto r^{-1/2}$ (from 1 to 10 AU) chosen to ensure Keplerian rotation.

22. For an axisymmetric, thin, collisionless disk, A. Toomre [*Astrophys. J.* **139**, 1217 (1964)] showed that a nonaxisymmetric perturbation will be unstable if $Q < 1$. Values of $Q \approx 1$ imply either marginal stability or instability. For a disk in Keplerian rotation, as is approximately the case here, Q is defined as $Q = 0.936 c_s \Omega / \pi G \sigma$, where c_s is the sound speed, Ω is the disk rotation rate, G is the gravitational constant, and σ is the surface (mass) density of the disk. For locally adiabatic variations in the disk temperature, the sound speed is defined as $c_s = (\gamma p / \rho)^{1/2}$.

23. G. W. Wetherill, *Annu. Rev. Earth Planet. Sci.* **18**, 205 (1990); *Icarus* **119**, 219 (1996).
24. A. P. Boss and E. A. Myhill, *Astrophys. J. Suppl. Ser.* **83**, 311 (1992).
25. A. P. Boss, *Lunar Planet. Sci. Conf.*, in press.
26. The Jeans mass is the mass of a sphere of uniform density gas with a radius equal to the Jeans length. The Jeans length is the critical wavelength necessary for self-gravitational collapse of an isothermal medium [L. Spitzer, *Diffuse Matter in Space* (Interscience, New York, 1968), p. 216]. In cgs units, the Jeans mass is given by $1.3 \times 10^{23} \, (T/\mu)^{3/2} \rho^{-1/2}$, where μ is the mean molecular weight.
27. The Lagrangian points define the region within which matter can be considered to be gravitationally bound to a planet in orbit about a star. The critical tidal radius is calculated by W. M. DeCampli and A. G. W. Cameron, *Icarus*, **38**, 367 (1979).

28. T. Velusamy, T. B. H. Kuiper, W. D. Langer, *Astrophys. J.* **451**, L75 (1995).
29. D. J. Stevenson and E. Fishbein, *Lun. Planet. Sci. Conf.* **XII** 1040 (1981).
30. S. J. Weidenschilling, in *Meteorites and the Early Solar System*, J. F. Kerridge and M. S. Matthews, Eds. (Univ. of Arizona Press, Tucson, 1988), pp. 348–371.
31. I thank S. Peale, G. Wetherill, and an anonymous referee for improvements to the manuscript. Supported in part by the Planetary Geology and Geophysics Program of NASA under grant NAG5-3873. Calculations were performed on the DEC Alpha workstations of the Carnegie Institution of Washington.

8 April 1997; accepted 7 May 1997

Oxygen on Ganymede: Laboratory Studies

R. A. Vidal,* D. Bahr, R. A. Baragiola,† M. Peters

To test proposals for the origin of oxygen absorption bands in the visible reflectance spectrum of Ganymede, the reflectance of condensed films of pure oxygen (O_2) and O_2-water mixtures and the evolution of O_2 from the films as a function of temperature were determined. Absorption band shapes and positions for oxygen at 26 kelvin were similar to those reported for Ganymede, whereas those for the mixtures were slightly shifted. The band intensity dropped by more than two orders of magnitude when the ice mixture was warmed to 100 kelvin, although about 20 percent of the O_2 remained trapped in the ice, which suggested that at these temperatures O_2 molecules dissolve in the ice rather than aggregate in clusters or bubbles. The experiments suggest that the absorption bands in Ganymede's spectrum were not produced in the relatively warm surface of the satellite but in a much colder source. Solid O_2 may exist in a cold subsurface layer or in an atmospheric haze.

Recent optical reflectance measurements of Ganymede revealed the presence of oxygen. Spencer *et al.* (*1*) found two weak absorption bands in the visible (at 5773 and 6275 Å) spectrum of Ganymede (but not of other icy satellites) that are signatures of interacting pairs of O_2 molecules (double transitions in adjacent molecules). In addition, Noll *et al.* (*2*) found a strong absorption band in the near ultraviolet (UV), which suggested the presence of condensed ozone. These oxygen signatures were prominent on Ganymede's trailing side, the side that is more subject to bombardment by ions from Jupiter's magnetosphere. This hemispheral difference led to suggestions that oxygen or ozone molecules originate either from direct implantation of oxygen ions into the surface or from radiolysis of ice, which accumulates beneath the surface

R. A. Vidal, D. Bahr, R. A. Baragiola, Laboratory for Atomic and Surface Physics, University of Virginia, Thornton Hall, Charlottesville, VA 22901, USA.
M. Peters, School of Medicine, Laboratory of Physics, Teikyo University, Ohtsuka 359, Hachioji-shi, Tokyo 192, Japan.

*Present address: Instituto de Tecnología Química, Güemes 3450, 3000 Santa Fé, Argentina.
†To whom correspondence should be addressed. E-mail: raul@virginia.edu

(*1–3*). However, the oxygen features were not seen in Europa's spectrum even though it is more heavily bombarded with ions and has been thought to have a denser oxygen atmosphere (*4*).

Ganymede's band positions were close to those previously measured for solid oxygen (*5*). To determine whether similar band positions result from condensed oxygen embedded in ice or other materials that may be present on Ganymede's surface, we measured optical reflectance spectra of pure solid oxygen, condensed O_2-H_2O mixtures, and irradiated ice. The experiments were made in a cryopumped ultrahigh-vacuum chamber (with a base pressure of $\sim 10^{-10}$ torr). We grew condensed gas films at ~ 13 Å/s by dosing degassed, pure water vapor or a 1:1 O_2-H_2O mixture onto the optically flat gold surface of a cooled quartz crystal microbalance. A quadrupole mass spectrometer measured the gas evolving from the films as they warmed up. The bidirectional reflectance was measured at a 90° phase angle and divided by the reflectance of a pure water ice film to remove the shape of the lamp spectrum and spectrometer efficiency function (*6, 7*).

The reflectance spectra of Ganymede

(*1*) are compared with the spectra of pure oxygen taken at the growth temperature 26 K (Fig. 1) (the films disappear in seconds if heated above 33 K). The absorption spectra, normalized for each band, obtained from Fig. 1 after the subtraction of the smooth continuum baselines are shown in Fig. 2. The position and shape of the bands for pure oxygen are similar to those observed on Ganymede and similar to those obtained in transmission experiments (*5*) for β-oxygen but are slightly shifted. To make a quantitative comparison, we estimated the optical path length L in our films as 2.4 times the film thickness, considering only single scattering events in the film and specular reflection at the substrate, because both absorption and scattering were weak. We obtained the absorption coefficient $\alpha(\lambda)$ at a wavelength λ from the decrease in reflectance $R(\lambda)$ due to absorption $R(\lambda) = 1 - \exp[-L\alpha(\lambda)]$. The integrated absorption coefficients $A = \int \alpha(\lambda)d\lambda$, given in Table 1 in mass units, agreed with previous reports (*5*) that used a density of 1.4 g/cm^3.

Spencer *et al.* (*1*) suggested that the oxygen on Ganymede is trapped in the ice, because at the minimum recorded daytime temperature on Ganymede, oxygen is liquid or gaseous with a vapor pressure (~ 75 mbar) that is orders of magnitude larger than the surface pressure upper limit implied by stellar occultation experiments (*8, 9*). Oxygen from a tenuous atmosphere could slowly accumulate in Ganymede's surface ice. Although it is known that microporous amorphous ice can trap gases efficiently below 110 K (*10*), the state of the trapped gas is not known; it can be in the form of gas bubbles in micropores or it may become dispersed into forms such as clathrate hydrates (*11*). This question can be addressed by looking at the optical bands due to O_2 pairs because their absorption strength depends on intermolecular distance (*12*).

We exposed a 17-μm-thick amorphous H_2O ice film to a flow of O_2 for 16 hours at

110 K to a total exposure of $\sim 10^{20}$ O_2 per cm^2. Consistent with a measured oxygen uptake of only $\lesssim 10^{17}$ O_2 per square centimeter, no O_2-O_2 absorption bands could be detected above the noise (0.25% band depth), which suggests that oxygen cannot be incorporated in ice at 110 K in amounts compatible with the observed band depths on Ganymede. Of course, we could not approach the levels of exposure that are possible on astronomical time scales from even a tenuous oxygen atmosphere. However, the oxygen uptake in those circumstances is actually expected to be lower because the micropores close due to the crystallization of ice, which should occur in times less than 2 years at temperature $T >$ 110 K, which is typical of Ganymede (6).

Ganymede's oxygen signature is variable. Spencer et al. (1) detected stronger bands in the western half of the satellite's orbit around Jupiter, which they interpreted as a difference between the surfaces of the leading and trailing hemispheres. They suggested that the greater flux of plasma ions into surface material on the trailing hemisphere either frees oxygen inside the ice by

dissociation of water molecules or directly implants energetic oxygen. Although it was found later that Ganymede's magnetic field is strong enough to deny jovian torus plasma direct access to Ganymede's surface other than at regions near the poles (13), we wanted to further test the ion bombardment hypothesis. We bombarded water ice with 50-keV $O_2{}^+$ ions but expected that this irradiation would not produce high oxygen concentrations because of the simultaneous removal of implanted oxygen by efficient sputtering [$\approx$60 H_2O molecules removed per incident $O_2{}^+$ (14)]. Nevertheless, we wanted to find out if a special configuration of O_2 molecules induced by irradiation might have an unusually high light absorption. We irradiated 100-μm water ice films grown at 20 K with 1.1×10^{17} O^+ per cm^2 at 100 K. To increase the amount of implanted oxygen beyond the limit allowed by sputtering, we divided the total irradiation into five periods and grew an additional 0.3 μm water film between them. The resulting irradiated layer had a average density of 3.5×10^{21} O per cm^3 and gave no detectable optical absorption.

As a way to force a high concentration of O_2 in water ice, we produced $\sim$1:1 O_2:H_2O gas mixtures and deposited films at $\sim$26 K to a total oxygen mass ranging from 1.2 to 9.6 mg/cm^2. To minimize fractionation, we grew the films in several increments, each time producing a fresh gas mixture. Thermal desorption experiments showed that the average O_2 concentration in the films was 42 to 67%. The band shapes measured at 26 K (Fig. 1) are similar to those of pure oxygen but are shifted to longer wavelengths. The relative strength of the bands varied from sample to sample, but their positions were reproducible to within a few angstroms. The absorption coefficients per oxygen molecule for the mixtures were close to those of pure oxygen (Table 1), which suggests that oxygen did not dissolve substantially but rather precipitated into aggregates. Because the absorption coefficient depends on density (12), the similarity of the values for the mixtures and pure oxygen implies that oxygen in the aggregates has a density similar to that of solid O_2. The shift in band positions between pure solid oxygen and the mixtures may be related to a different environment causing different phonon excitations during optical absorption (5). The band shapes for the mixtures are similar to those seen on Ganymede, but the agreement is not as good as for pure oxygen; also, the position of the 0-0 bands does not agree (Fig. 2).

These laboratory results were obtained at temperatures much lower than the diurnal surface temperatures at the satellite, which are 90 to 152 K (15). We thus warmed up the mixtures to 100 K and made further optical measurements. O_2 desorption was recorded with the mass spectrometer [water does not desorb significantly at those temperatures (6)], and the films were heated at a rate of 1.5 K per minute. The thermal desorption spectrum shown (Fig. 3)

Table 1. Band positions and absorption strengths for oxygen in different forms.

Reference	Band position (Å)		Integrated absorption A (10^{-6} cm^3/g)		Comment
	0-0 band	1-0 band	0-0 band	1-0 band	
Spencer et al. (1)	6275	5773 ± 1			Ganymede
This work, solid O_2	6274 ± 4	5762 ± 4	10 ± 1	8 ± 3	26 K
Landau et al. (5), solid O_2	6271 ± 4	5763 ± 1	28	26	α phase ($T <$ 23.9 K)
	6281 ± 8	5774 ± 7	7.6	6.9	β phase ($T >$ 23.9 K)
Dianov-Klokov (12), O_2 (solid and liquid)	6290	5769			β, γ, and liquid phases
Gas phase (35)	6300 ± 2	5772 ± 2			
This work, solid O_2:H_2O	6298 ± 6	5770 ± 4	10 ± 1	10 ± 2	26 K
			<0.6	<0.7	100 K

Fig. 1 (**left**). (Top) Reflectance spectra from Ganymede (1). (Bottom) Reflectance of 3.9 mg/ cm^2 of pure oxygen at 26 K (curve within circles) and 2.9 mg/cm^2 of a 0.72:1 O_2:H_2O film at 26 K (solid curve) and after warming up to 100 K (pluses). The curves are shifted for clarity. Fig. 2 (**right**). Normalized absorption bands for (**A**) 1-0 and (**B**) 0-0 for Ganymede (1) (dashed curve), pure oxygen (solid circles), and the 0.72:1 O_2:H_2O film mixture of Fig. 1 (solid curve with open circles.
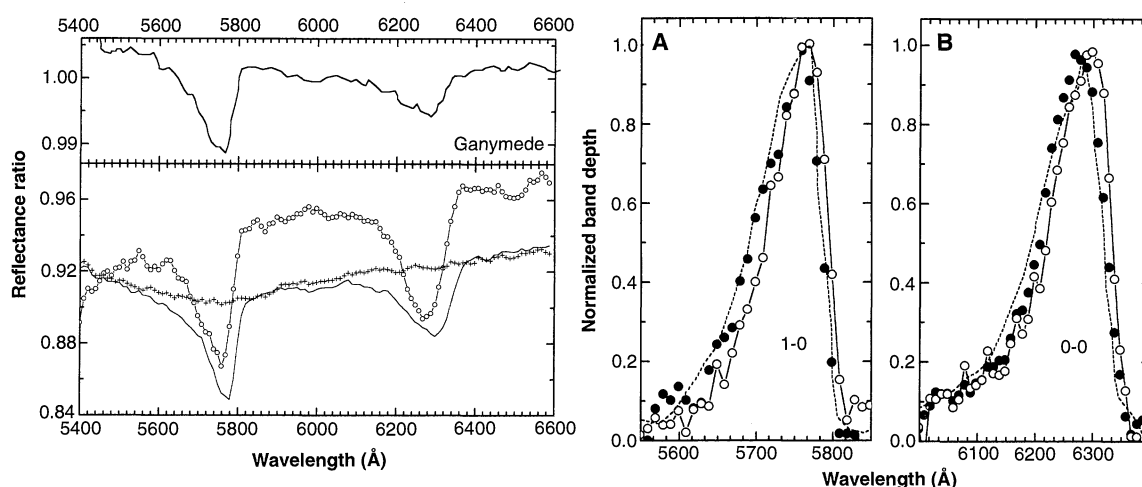
is very similar to those found for condensed Ar-H_2O mixtures (11, 16). After the films were warmed up to 100 K, the band intensities decreased by more than two orders of magnitude, below the noise level, although about 20% of the deposited oxygen remained in the ice. Because the absorption bands require two interacting O_2 molecules, we conclude that the oxygen remaining after warming is dissolved in the ice, rather than aggregated in, for example, bubbles in the films. Further heating to >130 K caused the ice to crystallize in seconds (6), releasing more than half of the remaining O_2 and peaking at 147 K. The desorption peak at ~165 K is likely related to the crystallization of the "restrained" amorphous ice form postulated recently (17), whereas O_2 desorption at higher temperatures is associated with the transformation into hexagonal ice (18) and the release of oxygen from clathrate hydrates formed during heating of the ice mixtures (19).

The upper limit of absorption strengths of O_2:H_2O ice mixtures at 100 K suggests that if this is the source of the oxygen bands on Ganymede, then the oxygen molecules need to be trapped over depths on the order of millimeters, depending on the degree of multiple scattering in the ice. Even larger depths would be needed if oxygen is not distributed uniformly over Ganymede's trailing hemisphere. However, such large depths would exceed the grain size–limited optical skin depth in Ganymede (20) and therefore contribute little to the measured visible reflectance. Our irradiation experiments with ions that were thought to be typical of the hot plasma bombarding Ganymede's trailing hemisphere (21) also showed no significant optical absorption. Implanted oxygen or oxygen produced by radiolysis with kiloelectron volt ions cannot directly produce the needed accumulation of oxygen at depths on the order of millimeters because the ions penetrate on the order of 1 μm or less. Diffusion to larger depths, on astronomical time scales, would further lower the oxygen concentration in the optical skin depth, which is already limited by sputtering, sublimation of the ice, and oxygen out-diffusion during irradiation, which is prominent above ~100 K (22). The hypothesis of trapped oxygen in Ganymede's surface ice cannot explain the observed spectral features for two reasons. First, oxygen cannot be absorbed or implanted in sufficient amounts to account for the strength of the observed bands. Second, the observed band shapes differ from those of the stable phases at the surface temperature: liquid or gaseous O_2, whose bands are more symmetric (12) than those observed on Ganymede and whose 0-0 band position falls several error bands outside that of the observed 0-0 band.

Thus, we need a colder source for the oxygen that produces Ganymede's visible bands. These bands are similar but slightly broader than those for pure oxygen at 26 K, which suggests a solid oxygen source at a temperature close to but below 55 K, the melting point of oxygen. Two possible sources are a cold subsurface layer and a haze of oxygen condensed from an oxygen atmosphere on cold particles, nucleating, for example, around dust from the jovian environment (23) or micrometeorite debris. A subsurface colder than daily temperatures has been inferred from thermal models of the surface regolith of galilean satellites (24), which explain the low thermal inertia shown by radiometry of eclipse transits (25). The models propose a porous layer (80 to 90% open space) a few millimeters thick, which is consistent with photometry results (26), overlaying a thermally conducting substrate. Average brightness temperatures as low as 55 ± 6 K for deeply probing 6-cm radiometry (27) translate into real temperatures of 60 to 80 K, as measured by radar albedos corrected for backscattering enhancement (28). Even colder regions will occur on patchy terrain. Oxygen can condense on the porous regolith at night, percolate down through the open surface structure, and possibly solidify. At dawn, the surface warms up, releasing oxygen from progressively deeper layers until possibly all the oxygen evaporates. This behavior is consistent with recent observations that condensed oxygen in the trailing hemisphere is present mainly at morning and evening longitudes (29). The time needed to evaporate all the subsurface oxygen will depend on flow restriction through narrow channels in the regolith and on the total amount of oxygen, which in turn will affect the thermal conductivity and inertia of the regolith. The thermal and structural properties of a particular terrain will determine the amount of oxygen trapped, and so it is not surprising that leading and trailing asymmetries and latitudinal variations result. This also means that the sublimating oxygen atmosphere will vary strongly depending on multiple factors such as the orbital position and time of day, the latitude, and the longitude.

If, on the other hand, all of Ganymede's daytime subsurface is too hot to harbor the solid oxygen needed to produce the observed absorption bands, the alternative is that solid oxygen particles exist in the atmosphere. There have been conflicting reports on the magnitude of an atmosphere on Ganymede. A stellar occultation in the red, seen from two locations on Earth, yielded a lower limit to surface pressure of 10^{-3} mbar. A Voyager occultation observa-

tion in the UV (9) gave instead an upper limit of 10^{-8} mbar for an atmosphere of gases that absorb significantly between 912 and 1700 Å but does not rule out a denser atmosphere of gases such as nitrogen and argon. Also, the 10^{-8}-mbar upper limit is one order of magnitude lower than the vapor pressure of water ice (6) at the highest day temperature observed (152 K) on Ganymede. Evidence supporting the presence of an atmosphere comes from the discovery of an ionosphere near Ganymede (30) and an aurora near its poles (31). Multiple sources for an oxygen atmosphere include photodesorption of ice from solar UV photons (32), direct sputtering, and photodissociation of desorbed or sputtered water molecules followed by hydrogen escape (33). An atmospheric pressure difference will circulate Ganymede's air from the day side to the night side, cooling the gas by adiabatic expansion as it rises to higher altitudes and as it moves laterally along the pressure gradient (34). Volatile species may cold-trap in a haze at altitudes and a range of latitudes at which the adiabatic cooling is strong and the heat inputs by plasma bombardment or solar UV are small (34). The haze may become optically thick to tangent rays and appear as an "atmospheric hard limb" during stellar occultation observations at UV and blue wavelengths, which possibly explains the contradictory occultation results (8, 9).

The cold-trapping haze should be variable because the rate at which gases sublimate on the day side depends on heat input, and thus the day side atmospheric pressure will be higher at jovian perihelion and also when Ganymede's day side faces Jupiter. Other orbital variations may result from drastic changes in the circulation of the atmosphere caused by the jovian eclipse: Sublimation will be reduced, gas will condense on the day side, and the haze will warm up as it radiatively equilibrates and could sublimate completely. Jovian eclipses may be a source of the orbital variability of the condensed O_2 bands if time scales are
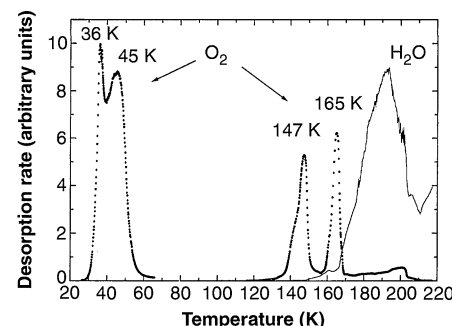

Fig. 3. Thermal desorption spectra for a 0.96:1 O_2:H_2O film at a heating rate of 1.5 K/min.

sufficiently long for the regeneration of an atmospheric haze cold enough to condense O_2 after an eclipse. The present laboratory results provide a rationale for assessing the possibility of a variable sublimation-driven atmosphere and haze that are cold enough to condense O_2.

REFERENCES AND NOTES

1. J. R. Spencer, W. M. Calvin, M. J. Person, *J. Geophys. Res.* **100**, 19049 (1995); W. M. Calvin, R. E. Johnson, J. R. Spencer, *Geophys. Res. Lett.* **23**, 673 (1996).
2. K. S. Noll, R. E. Johnson, A. L. Lane, D. L. Domingue, H. A. Weaver, *Science* **273**, 341 (1996).
3. R. E. Johnson and W. A. Jesser, *Astrophys. J. Lett.*, **480**, 1 (1997).
4. D. T. Hall et al., *Nature* **373**, 677 (1995).
5. A. Landau, E. J. Allin, H. L. Welsh, *Spectrochim. Acta* **18**, 1 (1962).
6. N. J. Sack and R. A. Baragiola, *Phys. Rev. B* **48**, 9973 (1993). The microbalance can be used for films thinner than ~ 10 μm; for thicker films, the amount of condensed gas is determined by thermal desorption mass spectrometry, calibrated against the microbalance to within 10%.
7. N. J. Sack et al., *J. Geophys. Res.* **96**, 17535 (1991). Collimated light from a quartz halogen lamp was incident at 35° to the sample normal; light scattered at 55° to the normal was analyzed by a grating spectrometer at a resolution of 20 Å, with a wavelength scale calibrated with the use of a Hg reference lamp.
8. R. W. Carlson et al., *Science* **182**, 53 (1973).
9. A. L. Broadfoot et al., *ibid.* **204**, 979 (1979).
10. E. Mayer and R. Pletzer, *Nature* **319**, 298 (1986).
11. A. Bar-Nun et al., *Phys. Rev.* **35**, 2427 (1987).
12. V. I. Dianov-Klokov, *Opt. Spectrosc.* **XIII**, 109 (1962).
13. M. Kivelson et al., *Nature* **384**, 537 (1996).
14. M. Shi et al., *Nucl. Instrum. Methods* **B96**, 524 (1995).
15. G. S. Orton, J. R. Spencer, L. D. Travis, T. Z. Martin, L. K. Tamppari, *Science* **274**, 389 (1996).
16. The desorption peak at 36 K is attributed to the evaporation of solid oxygen; the peak at 45 K is attributed to multilayers of oxygen in slightly stronger binding sites, such as cracks in the ice (11).
17. P. Jenniskens and D. F. Blake, *Science* **265**, 753 (1994).
18. L. G. Dowell and A. P. Rinfret, *Nature* **188**, 1144 (1960).
19. D. Blake, L. Allamandola, S. Sanford, D. Hudgins, F. Freund, *Science* **254**, 548 (1991).
20. R. N. Clark, *Icarus* **44**, 388 (1980).
21. After this work was finished, M. Kivelson et al. (13) found that Ganymede has a magnetic field strong enough to prevent direct access of the jovian torus plasma to Ganymede's surface other than at regions near the poles.
22. C. T. Reimann et al., *Surf. Sci.* **147**, 227 (1984); A. Bar-Nun et al., *ibid.* **150**, 143 (1985).
23. E. Grun et al., *Nature* **381**, 395 (1996).
24. D. L. Matson and D. B. Nash, *J. Geophys. Res.* **88**, 4771 (1983); D. L. Matson and R. H. Brown, *Icarus* **77**, 67 (1989); M. L. Urquhart and B. M. Jakosky, *J. Geophys. Res.* **101**, 21,169 (1996).
25. D. Morrison and D. P. Cruikshank, *Icarus* **18**, 224 (1973); O. L. Hansen, *ibid.*, p. 237.
26. B. J. Buratti, *ibid.* **92**, 312 (1991).
27. I. de Pater, R. A. Brown, J. R. Dickel, *ibid.* **57**, 93 (1984). Their temperatures were calculated with uncorrected radar albedos.
28. Enhancement of 1.5 to 2 can be derived from M. I. Mishchenko [*J. Quant. Spectrosc. Radiat. Transfer* **56**, 673 (1996)].
29. W. Calvin and J. Spencer, in preparation.
30. D. A. Gurnett, W. S. Kurth, A. Roux, S. J. Bolton, C. F. Kennel, *Nature* **384**, 535 (1996).
31. D. T. Hall, P. D. Feldman, M. A. McGrath, D. F. Strobel, in preparation.
32. M. S. Westley, R. A. Baragiola, R. E. Johnson, G. A. Baratta, *Nature* **373**, 405 (1995); *Planet. Space Sci.* **43**, 1311 (1995).
33. Y. L. Yung and M. B. McElroy, *Icarus* **30**, 97 (1977); S. Kumar and D. M. Hunten, in *Satellites of Jupiter*, D. Morrison, Ed. (Univ. of Arizona Press, Tucson, AZ, 1982), pp. 782–806.
34. The low temperatures attainable by sublimation atmospheres, below 30 K, were shown by models of SO_2 on Io for various combinations of upward and lateral gas movement in the absence of plasma heating [M. A. Moreno et al., *Icarus* **93**, 63 (1991); M. Wong and R. E. Johnson, *ibid.* **115**, 109 (1995)]. We ignored plasma heating because the ion flux should be much reduced in Ganymede because of its magnetic field (13), and heating by solar ultraviolet and infrared radiation is neglected because the absorption cross sections for O_2 are very low (orders of magnitude lower than for SO_2).
35. G. D. Greenblatt et al., *J. Geophys. Res.* **95**, 18577 (1990).
36. We thank R. E. Johnson and B. Donn for stimulating discussions. Supported by NASA and NSF. R.A.V. acknowledges support from the Consejo Nacional de Investigaciones Científicase y Técnicas of Argentina and Fundación Antorchas.

20 March 1997; accepted 5 May 1997

Requirement of Guanosine Triphosphate–Bound Ran for Signal-Mediated Nuclear Protein Export

Stephanie A. Richards,* Kimberly L. Carey, Ian G. Macara†

A leucine-rich nuclear export signal (NES) allows rapid export of proteins from cell nuclei. Microinjection studies revealed a role for the guanosine triphosphatase (GTPase) Ran in NES-mediated export. Nuclear injection of a Ran mutant ($\text{Thr}^{24} \rightarrow \text{Asn}$) blocked protein export but not import, whereas depletion of the Ran nucleotide exchange factor RCC1 blocked protein import but not export. However, injection of Ran GTPase-activating protein (RanGAP) into RCC1-depleted cell nuclei inhibited export. Coinjection with Ran mutants insensitive to RanGAP prevented this inhibition. Therefore, NES-mediated protein export appears to require a Ran-GTP complex but does not require Ran-dependent GTP hydrolysis.

Bidirectional movement of proteins across the nuclear membrane occurs through the nuclear pore complex. Import of nuclear proteins containing a nuclear localization signal (NLS) requires the small GTPase Ran and associated proteins (1). The process of nuclear protein export is less well understood, but the recent identification of NESs suggests that NES-specific receptors are likely involved. Related NESs have been identified in Ran binding protein 1 (RanBP1) (2), protein kinase A inhibitor, mitogen-activated protein kinase kinase, the yeast protein Gle1p, and the retroviral proteins Rev and Rex (3).

To examine the role of Ran in nuclear protein export, we constructed an export substrate, GGNES, that contained glutathione-S-transferase (GST) attached to green fluorescent protein (GFP) and the RanBP1 NES (Lys-Val-Ala-Glu-Lys-Leu-Glu-Ala-Leu-Ser-Val-Arg, residues 178 to 189) (4). At 55 kD, this substrate is too large to diffuse passively through the nuclear pores within the experimental time frame. GGNES and GG (a GST-GFP construct lacking the NES) were each ex-

S. A. Richards and K. L. Carey, Department of Pathology, University of Vermont, Burlington, VT 05405, USA.
I. G. Macara, Center for Cell Signaling, Box 577, Health Sciences Center, University of Virginia, Charlottesville, VA 22908, USA.

*Present address: Department of Cell Biology, Harvard Medical School, Boston, MA 02115, USA.
†To whom correspondence should be addressed. E-mail: igm9c@virginia.edu

pressed in *Escherichia coli*, purified, and injected into nuclei of baby hamster kidney cells (BHK21); fluorescent dextran marked the injection site (5). After a 60-min incubation, the GG and GGNES proteins were visualized by epifluorescence microscopy. The GG control remained nuclear after injection, but the GGNES substrate was exported to the cytoplasm (Fig. 1A). To determine the rate of GGNES export, we incubated injected cells for various intervals before fixation and analysis (6). GGNES export was essentially complete by 15 min (Fig. 1B).

To further examine the role of Ran in NES-dependent nuclear protein export, we coinjected selected Ran mutants with GGNES. Mutants were chosen that were expected to display dominant phenotypes. A mutant in which Gly^{19} was replaced by Val (Ran G19V) is insensitive to the Ran nucleotide exchange factor, RCC1, and to the Ran GTPase-activating protein, RanGAP; it is predominantly in an active, GTP-bound form in BHK21 cells (7). Ran T24N ($\text{Thr}^{24} \rightarrow \text{Asn}$) does not bind nucleotide stably and exhibits increased affinity for RCC1 (7, 8). Ran E46G ($\text{Glu}^{46} \rightarrow \text{Gly}$) has a mutation in the effector domain, which is thought to mediate interactions with downstream target proteins. The E46G mutant is insensitive to RanGAP but undergoes RCC1-mediated nucleotide exchange, which suggests that it is GTP-bound in the cell (7).